DOI: 10.1021/ic901083u

Inorganic Chemistry
Article

Nickel(II) Complexes of Monofunctionalized Pyridine-Azamacrocycles: Synthesis, Structures, Pendant Arm "On-Off" Coordination Equilibria, and Peroxidase-like Activity

Voltaire G. Organo,[†,§] Alexander S. Filatov,[‡] Justin S. Quartararo,[†] Zachary M. Friedman,[†] and Elena V. Rybak-Akimova*[,†]

[†]*Department of Chemistry, Tufts University, Medford, Massachusetts 02155,* [‡]*Department of Chemistry, University at Albany, SUNY, Albany, New York 12222, and* [§]*Department of Physical Sciences and Mathematics, University of the Philippines, Manila 1000, Philippines*

Received June 4, 2009

Novel nickel(II) complexes of pyridine-azamacrocycles (PyMACs) with pendant arms have been synthesized using simple, direct, and selective mono-*N*-functionalization of PyMACs. These complexes have been characterized by spectroscopy and X-ray crystallography. Nickel(II)-PyMAC complexes with a flexible pendant arm bearing a tertiary amine, a carboxylic acid, or an amide group exhibit structural and color changes due to "on-off" arm coordination to the metal center. Five- or six-coordinate complexes with the arm bound to the nickel(II) center are high-spin, while their four-coordinate "arm-off" counterparts are low-spin. Synergistic axial coordination of acetonitrile and the amide group from the pendant arm was observed. Coordination to the nickel(II) center lowers the pK_a of the functional group attached to the macrocycle via a propylene linker by up to 4−5 orders of magnitude. Varying hydrogen bonding and proton-donating properties of the pendant arm affects the peroxidase-like activity of Ni(II)-PyMAC complexes in the oxidation of ABTS with hydrogen peroxide.

Introduction

Macrocycles with pendant arms have attracted interest in recent years owing to their unique coordination and structural properties, and their wide utility in synthetic chemistry, biology, and medicine.[1] Pendant arms can serve different roles depending on the nature of their functional groups. For example, electron-donating pendant arms can serve as additional ligands to bound metal ions. This causes their metal complexes to be more thermodynamically and kinetically stable, which is important in developing radiopharmaceutical drugs and magnetic resonance imaging agents.[2] Coordination of the pendant arm to transition metal ions can also alter redox properties of the metal and allows stabilization of unusual oxidation states.[3] Pendant arms of metallomacrocycles can also be utilized in molecular recognition of substrates via noncovalent, intermolecular interactions such as hydrogen bonding, hydrophilic or hydrophobic interaction.[4,5] They can also act as Brønsted-Lowry acids for proton-coupled

*To whom correspondence should be addressed. E-mail: elena.rybak-akimova@tufts.edu.

(1) Archibald, S. J. *Annu. Rep. Prog. Chem., Sect. A* **2008**, *104*, 272–296. Kimura, E. *Tetrahedron* **1992**, *48*, 6175–6217. Fabbrizzi, L.; Foti, F.; Licchelli, M.; Poggi, A.; Taglietti, A.; Vazquez, M. *Adv. Inorg. Chem.* **2007**, *59*, 81–107.

(2) Aime, S.; Gianolio, E.; Corpillo, D.; Cavallotti, C.; Palmisano, G.; Sisti, M.; Giovenzana, G. B.; Pagliarin, R. *Helv. Chim. Acta* **2003**, *86*, 615–632. Kong, D.; McBee, J.; Holliness, L.; Clearfield, A. *Tetrahedron Lett.* **2008**, *49*, 3512–3515. Smith, S. V. *J. Inorg. Bio.* **2004**, *98*, 1874–1901. Cacheris, W. P.; Nickle, S. K.; Sherry, A. D. *Inorg. Chem.* **1987**, *26*, 958–960. Bernhardt, P. V.; Sharpe, P. C. *Inorg. Chem.* **2000**, *39*, 4123–4129. Chappell, L. L.; David, A.; Voss, J.; Horrocks, W. D.; Morrow, J. R. *Inorg. Chem.* **1998**, *37*, 3989–3998. Lewis, E. A.; Boyle, R. W.; Archibald, S. J. *Chem. Commun.* **2004**, 2212–2213. Lewis, M. R.; Wang, M.; Axworthy, D. B.; Theodore, L. J.; Mallet, R. W.; Fritzberg, A. R.; Welch, M. J.; Anderson, C. J. *J. Nucl. Med.* **2003**, *44*, 1284–1292. Silversides, J. D.; Allan, C. C.; Archibald, S. J. *Dalton Trans.* **2007**, 971–978. Marques, F.; Guerra, K. P.; Gano, L.; Costa, J.; Campello, M. P.; Lima, L. M. P.; Delgado, R.; Santos, I. *J. Biol. Inorg. Chem.* **2004**, *9*, 859–872. Siaugue, J.-M.; Segat-Dioury, F.; Favre-Reguillon, A.; Madic, C.; Foos, J.; Guy, A. *Tetrahedron Lett.* **2000**, *41*, 7443–7446.

(3) Bukowski, M. R.; Koehntop, K. D.; Stubna, A.; Bominaar, E. L.; Halfen, J. A.; Münck, E.; Nam, W.; Que, L., Jr. *Science* **2005**, *310*, 1000–1002. Kimura, E. *Pure Appl. Chem.* **1986**, *58*, 1461–1466. Kimura, E.; Joko, S.; Koike, T.; Kodama, M. *J. Am. Chem. Soc.* **1987**, *109*, 5528–5529. Grapperhaus, C. A.; Mienert, B.; Bill, E.; Weyhermuller, T.; Wieghardt, K. *Inorg. Chem.* **2000**, *39*, 5306–5317. Nam, W. *Acc. Chem. Res.* **2007**, *40*, 522–531. Sastri, C. V.; Lee, J.; Oh, K.; Lee, Y. J.; Lee, J.; Jackson, T. A.; Ray, K.; Hirao, H.; Shin, W.; Halfen, J. A.; Kim, J.; Que, L., Jr.; Shaik, S.; Nam, W. *Proc. Natl. Acad. Sci.* **2007**, *104*, 19181–19186.

(4) Benniston, A. C.; Gunning, P.; Peacock, R. D. *J. Org. Chem.* **2005**, *70*, 115–123. Yang, J.; Breslow, R. *Angew. Chem., Int. Ed.* **2000**, *39*, 2692–2695. Yang, J.; Gabriele, B.; Belvedere, S.; Huang, Y.; Breslow, R. *J. Org. Chem.* **2002**, *67*, 5057–5067. Breslow, R.; Singh, S. *Bioorg. Chem.* **1988**, *16*, 408–417.

(5) Reichenbach-Klinke, R.; Konig, B. *J. Chem. Soc., Dalton Trans.* **2002**, 121–130. Das, S.; Incarvito, C. D.; Crabtree, R. H.; Brudvig, G. W. *Science* **2006**, *312*, 1941–1943. Hull, J. F.; Sauer, E. L. O.; Incarvito, C. D.; Faller, J. W.; Brudvig, G. W.; Crabtree, R. H. *Inorg. Chem.* **2009**, *48*, 488–495 and references therein.

Published on Web 08/11/2009

redox reactions.[6−8] Moreover, pendant arms can be used to covalently link macrocycles or metallomacrocycles to solid supports,[9] fluorophores,[10] and biomolecules.[11] Such functionalized macrocycles are useful in biomimetic studies, imaging, sensing, and catalysis.

Macrocycles with a single pendant arm are particularly attractive ligands for studying the effects of pendant arms on the properties of the metal ion incorporated within the macrocyclic ring. Their coordination chemistry is simpler compared to macrocycles with multiple arms,[12,13] albeit their synthesis is less straightforward. Single-site attachment of a pendant arm onto azamacrocycles poses a challenge because of the presence of several equivalent −NH groups which can potentially lead to multiple products with varying degrees of *N*-alkylation. Several synthetic methodologies have been reported toward selective mono-*N*-alkylation of azamacrocycles.[13−16] On the other hand, those dealing with the synthesis of pyridine-containing azamacrocycles (PyMACs) with single pendant arms are few, even though PyMACs possess intrinsic asymmetry which makes them particularly suitable for mono-functionalization.

We[17,18] and others[19−22] have developed strategies to prepare macrocycles with single pendant arms based on aminopyridines. One approach requires a multistep synthesis of the polyamine precursor prior to cyclization with a dihaloalkyl- or diacyl-pyridine derivative. Another approach involves a direct metal-template condensation reaction of 2,6-diformyl or diacetylpyridine with a tripodal amine to produce a macrocyclic ligand bearing an amine pendant arm. This unique ligand now contains a functional group which can be modified to vary properties of the arm such as hydrogen bonding and electron pair donating ability. This strategy, however, is limited to derivatization of the amine pendant arm. This led us to develop practical approaches in introducing functionalized pendant arms into pyridine-azamacrocycles. We are particularly interested in incorporating functional groups with different acid/base and hydrogen bonding properties.

Here we report simple, convenient and selective synthetic methodologies for preparing PyMACs bearing either a carboxylic acid, an amide, or a tertiary amine pendant arm. Their nickel(II) complexes have been prepared and characterized by spectroscopy and X-ray crystallography. Acid−base equilibria and arm "on-off" coordination equilibria were investigated in solution. We also report the unexpected peroxidase-like activity of these nickel complexes and demonstrate the effect of varying pendant arms on the catalytic behavior of the complexes.

Experimental Section

General Considerations. Reagents were obtained from commercially available sources and used without further purification. Ligand **Lb**,[17,23] and complexes [Ni(**LNH$_2$**)](ClO$_4$)$_2$,[17] [Ni(**LNHCOMe**)](ClO$_4$)$_2$,[17,24] and [Ni(**LMe**)](ClO$_4$)$_2$[23] were prepared as described elsewhere. UV−vis spectra were acquired on a Jasco V-570 spectrophotometer. IR spectra were recorded on a Thermo FTIR-100 spectrometer. ^{1}H and ^{13}C NMR spectra were recorded on a Bruker DPX-300 MHz spectrometer. Elemental analyses were performed by Schwarzkopf Microanalytical Laboratory (Woodside, NY) and Robertson Microlit Laboratories (Madison, NJ).

Caution! *Perchlorate salts of metal complexes with organic ligands are potentially explosive. Only small amounts of material should be prepared, and these should be handled with great caution.*

Reductive Alkylation of [Ni(LNH$_2$)](ClO$_4$)$_2$. Acetaldehyde (1.0 mL, 17 mmol) was added to the MeCN-MeOH (1:1) solution of [Ni(**LNH$_2$**)](ClO$_4$)$_2$ (1.0 g, 1.7 mmol) and stirred for 10 min. NaBH$_3$CN (0.22 g, 3.5 mmol) was then added, and the mixture stirred at room temperature (RT) overnight. Afterward, the solution was rotavaped to dryness. The residue was dissolved in MeNO$_2$, filtered, and rotavaped to dryness. The residue was redissolved in MeCN and poured into toluene. After several days, pink crystals grew and were characterized as [**NiLNEt$_2$**](**BH$_3$CN**)$_2$.

(6) Chang, C. J.; Chng, L. L.; Nocera, D. G. *J. Am. Chem. Soc.* **2003**, *125*, 1866–1876.
(7) Dempsey, J. L.; Esswein, A. J.; Manke, D. R.; Rosenthal, J.; Soper, J. D.; Nocera, D. G. *Inorg. Chem.* **2005**, *44*, 6879–6892.
(8) Soper, J. D.; Kryatov, S. V.; Rybak-Akimova, E. V.; Nocera, D. G. *J. Am. Chem. Soc.* **2007**, *129*, 5069–5075.
(9) Blanco, B.; Moreno-Mañas, M.; Pleixats, R.; Mehdi, A.; Reyé, C. *J. Mol. Catal. A: Chem.* **2007**, *269*, 204–213. Bonora, G. M.; Drioli, S.; Felluga, F.; Mancin, F.; Rossi, P.; Scrimin, P.; Tecilla, P. *Tetrahedron Lett.* **2003**, *44*, 535–538. Brulé, E.; de Miguel, Y. R.; Hii, K. K. *Tetrahedron* **2004**, *60*, 5913–5918. Zhang, J.-L.; Che, C.-M. *Org. Lett.* **2002**, *4*, 1911–1914.
(10) Blake, A. J.; Bencini, A.; Caltagirone, C.; Filippo, G. D.; Dolci, L. S.; Garau, A.; Isaia, F.; Lippolis, V.; Mariani, P.; Prodi, L.; Montalti, M.; Zaccheroni, N.; Wilson, C. *Dalton Trans.* **2004**, 2771–2779. Koike, T.; Watanabe, T.; Aoki, S.; Kimura, E.; Shiro, M. *J. Am. Chem. Soc.* **1996**, *118*, 12696–12703. Tamanini, E.; Katewa, A.; Sedger, L. M.; Todd, M. H.; Watkinson, M. *Inorg. Chem.* **2009**, *48*, 319–324.
(11) De Leon-Rodriguez, L. M.; Kovacs, Z. *Bioconjugate Chem.* **2008**, *19*, 391–402. Kaden, T. A.; Tschudin, D.; Studer, M.; Brunner, U. *Pure Appl. Chem.* **1989**, *61*, 879–883.
(12) Tschudin, D.; Basak, A.; Kaden, T. A. *Helv. Chim. Acta* **1988**, *71*, 100–106.
(13) Wainwright, K. P. *Coord. Chem. Rev.* **1997**, *166*, 35–90.
(14) Alcock, N. W.; McLaren, F.; Moore, P.; Pike, G. A.; Roe, S. M. *J. Chem. Soc., Chem. Commun.* **1989**, 629–632. Bernard, H.; Yaouanc, J. J.; Clément, J. C.; des Abbayes, H.; Handel, H. *Tetrahedron Lett.* **1991**, *32*, 639–642. Boschetti, F.; Denat, F.; Espinosa, E.; Lagrange, J.-M.; Guilard, R. *Chem. Commun.* **2004**, 588–589. Boschetti, F.; Denat, F.; Espinosa, E.; Tabard, A.; Dory, Y.; Guilard, R. *J. Org. Chem.* **2005**, *70*, 7042–7053. Chuburu, F.; Le Baccon, M.; Handel, H. *Tetrahedron* **2001**, *57*, 2385–2390. Fensterbank, H.; Zhu, J.; Riou, D.; Larpent, C. *J. Chem. Soc., Perkin Trans. 1* **1999**, 811–815. Hediger, M.; Kaden, T. A. *Helv. Chim. Acta* **1983**, *66*, 861–870. Kang, S.-G.; Kim, S.-J.; Ryu, K.; Kim, J. *Inorg. Chim. Acta* **1998**, *274*, 24–31. Krivickas, S. J.; Tamanini, E.; Todd, M. H.; Watkinson, M. *J. Org. Chem.* **2007**, *72*, 8280–8289. Li, C.; Wong, W.-T. *Tetrahedron Lett.* **2002**, *43*, 3217–3220. Massue, J.; Plush, S. E.; Bonnet, C. S.; Moore, D. A.; Gunnlaugsson, T. *Tetrahedron Lett.* **2007**, *48*, 8052–8055. Meunier, I.; Mishra, A. K.; Hanquet, B.; Cocolios, P.; Guilard, R. *Can. J. Chem.* **1995**, *73*, 685–695. Patinec, V.; Yaouanc, J. J.; Clement, J. C.; Handel, H.; des Abbayes, H. *Tetrahedron Lett.* **1995**, *36*, 79–82. Rawle, S. C.; Clarke, A. J.; Moore, P.; Alcock, N. W. *J. Chem. Soc., Dalton Trans.* **1992**, 2755–2757. Skwierawska, A. M. *Tetrahedron Lett.* **2008**, *49*, 6308–6310. Turonek, M. L.; Moore, P.; Clase, H. J.; Alcock, N. W. *J. Chem. Soc., Dalton Trans.* **1995**, 3659–3666. Yaouanc, J.-J.; Le Bris, N.; Le Gall, G.; Clement, J.-C.; Handel, H.; des Abbayes, H. J. *Chem. Soc., Chem. Commun.* **1991**, 206–207.
(15) Pallavicini, P. S.; Perotti, A.; Poggi, A.; Seghi, B.; Fabbrizzi, L. *J. Am. Chem. Soc.* **1987**, *109*, 5139–5144.
(16) Studer, M.; Kaden, T. A. *Helv. Chim. Acta* **1986**, *69*, 2081–2086.
(17) Herrera, A. M.; Staples, R. J.; Kryatov, S. V.; Nazarenko, A. Y.; Rybak-Akimova, E. V. *Dalton Trans.* **2003**, 846–856.
(18) Rybak-Akimova, E. V.; Nazarenko, A. Y.; Silchenko, S. S. *Inorg. Chem.* **1999**, *38*, 2974–2980.
(19) Alcock, N. W.; Balakrishnan, K. P.; Moore, P.; Omar, H. A. A. *J. Chem. Soc., Dalton Trans.* **1987**, 545–550.
(20) Alcock, N. W.; Kingston, R. G.; Moore, P.; Pierpoint, C. *J. Chem. Soc., Dalton Trans.* **1984**, 1937–1943.
(21) Grant, S. J.; Moore, P.; Omar, H. A. A.; Alcock, N. W. *J. Chem. Soc., Dalton Trans.* **1994**, 485–489. An, H.; Cummins, L. L.; Griffey, R. H.; Bharadwaj, R.; Haly, B. D.; Fraser, A. S.; Wilson-Lingardo, L.; Risen, L. M.; Wyatt, J. R.; Cook, P. D. *J. Am. Chem. Soc.* **1997**, *119*, 3696–3708. Dioury, F.; Sylvestre, I.; Siague, J.-M.; Wintgens, V.; Ferroud, C.; Favre-Reguillon, A.; Foos, J.; Guy, A. *Eur. J. Org. Chem.* **2004**, 4424–4436.
(22) Lotz, T. J.; Kaden, T. A. *Helv. Chim. Acta* **1978**, *61*, 1376–1387.
(23) Rusnak, L.; Jordan, R. B. *Inorg. Chem.* **1971**, *10*, 2199–2204.
(24) Ye, W.; Rybak-Akimova, E. V., *Manuscript in preparation.*

Yield (0.51 g, 57%). IR (solid): ν (cm^{-1}) = 3248, 2371, 2338, 2274, 2189, 1115; ESI-MS (+): m/z = 514.18 ({[Ni(LNEt$_2$)](BH$_3$CN)$_2$ +H}$^+$, 100%), 473.36 ({[Ni(LNEt$_2$)](BH$_3$CN)}$^+$, 80%). Anal. Calcd for $C_{24}H_{47}B_2N_7Ni\cdot H_2O$: C 54.18%, H 9.28%, N 18.43%; found: C 53.72%, H 9.17%, N 18.10%.

Synthesis of [Ni(LNEt$_2$)](ClO$_4$)$_2$ and [Ni(HLNEt$_2$)](ClO$_4$)$_3$. Same as the above procedure except that after overnight reaction and removing the solvent, the residue was dissolved in MeOH, acidified to pH ~ 4 with $HClO_4$ (70% in H_2O), and then placed in the freezer overnight. The orange precipitate formed was filtered and recrystallized in cold ethanol. Single-crystals of the complex suitable for X-ray diffraction were grown from slow diffusion of diethyl ether into an acetonitrile solution of the complex. Yield (79%). ESI-MS(+): m/z = 432.36 ({[Ni-(LNEt$_2$)]-H}$^+$, 100%), 216.73 ({[Ni(LNEt$_2$)]}$^{2+}$, 95%), 532.27 ({[Ni(LNEt$_2$)](ClO$_4$)}$^+$, 10%); Anal. Calcd for $C_{22}H_{41}Cl_2N_5NiO_8\cdot 0.7H_2O$: C 40.92%, H 6.62%, 10.84%; found: C 40.98%, H 6.78%, N 10.88%. [Ni(HLNEt$_2$)](ClO$_4$)$_3$ can be prepared by acidifying a methanolic solution of [Ni(LNEt$_2$)](ClO$_4$)$_2$ to pH~ 3 with $HClO_4$. After removing the solvent, the oily orange product was dissolved in MeCN and treated with ethyl acetate. Single crystals of the protonated complex formed after slow evaporation of the solvent mixture. Yield (94%). ESI-MS (+): m/z = 634.18 ({[Ni(HLNEt$_2$)](ClO$_4$)$_2$}$^+$, 100%), 532.27 ({[Ni(LNEt$_2$)]ClO$_4$}$^+$, 44%); Anal. Calcd for $C_{22}H_{42}Cl_3N_5NiO_{12}$: C 36.02%, H 5.77%, N 9.55%; found: C 36.16%, H 6.04%, N 9.25%.

Synthesis of LNEt$_2$. To [Ni(**LNEt$_2$**)](ClO$_4$)$_2$ (0.44 g, 0.69 mmol) dissolved in 10 mL of warm water was added NaCN (0.24 g, 4.8 mmol) and stirred for 1 h. The ligand was extracted with $CHCl_3$ (3×10 mL). The combined organic layer was washed with brine, dried over Na_2SO_4 then rotavaped to dryness yielding a yellowish oil. Yield (0.19 mg, 75%); IR (neat): ν (cm^{-1}) = 3265, 1573; ESI-MS(+): m/z = 398.55 ({LNEt$_2$+Na}$^+$, 100%), 376.55 ({LNEt$_2$+H}$^+$, 15%); ^{1}H NMR (300 MHz, $CDCl_3$, 300K): δ = 7.48 (t, J = 7.5 Hz, 1H), 6.88 (d, J = 7.5 Hz, 2H), 3.64 (q, J = 6.9 Hz, 2H), 2.80 (br. s, 2H), 2.44−2.10 (m, 16H), 1.67−1.45 (m, 6H), 1.32 (d, J = 7.2 Hz, 6H), 0.93 (t, J = 7.2 Hz, 6H); ^{13}C NMR (300 MHz, $CDCl_3$, 300K): δ = 164.20, 136.09, 120.26, 59.32, 51.25, 51.17, 46.87, 45.25, 27.31, 23.90, 23.57, 11.69.

Synthesis of LCOOH. To a 20 mL aqueous solution of **Lb** (0.50 g, 1.9 mmol) was added acrylic acid (0.13 mL, 2.1 mmol), and the mixture stirred at 70 °C under N_2 for 24 h. After cooling to RT, the aqueous solution was treated with NH_4OH (2 mL). Unreacted ld > Lb was extracted with $CHCl_3$ (5 ×25 mL). The aqueous layer was evaporated to dryness under vacuum. The oily residue was dissolved in EtOH, treated with diethyl ether, and placed in the freezer overnight to afford a white solid. Yield (0.45 mg, 71%); IR (solid): ν (cm^{-1}) = 3469, 1610, 1548, 1372; ESI-MS(+): m/z = 335.36 ({LCOOH+H}$^+$, 100%); ^{1}H NMR (300 MHz, D_2O, 300K): δ = 7.83 (t, J = 7.8 Hz, 1H), 7.32 (d, J = 7.8 Hz, 2H), 4.50 (q, J = 6.9 Hz, 2H), 2.96−2.81 (m, 4H), 2.55−2.48 (m, 4H), 2.37−2.27 (m, 2H), 2.17 (t, J = 6.3 Hz, 2H), 1.86 (m, J = 5.4 Hz, 4H), 1.50 (d, J = 6.3 Hz, 6H); ^{13}C NMR (300 MHz, D_2O, 300K): δ = 181.33, 155.06, 139.87, 122.86, 58.68, 49.80, 49.14, 44.84, 33.61, 22.60, 19.78.

Synthesis of [Ni(LCOOH)](ClO$_4$)$_2$. Ni(ClO$_4$)$_2\cdot$6H$_2$O (64 mg, 0.18 mmol) was added to a methanol solution of LCOOH (58 mg, 17 mmol), stirred and refluxed for 30 min. After removing the solvent, the orange residue was dissolved in MeCN. Slow diffusion of diethyl ether into this solution yielded dark orange crystals which were filtered, washed with diethyl ether, and dried in air. Yield (80 mg, 77%); IR (solid): ν (cm^{-1}) = 3426, 1726, 1054; ESI-MS (+): m/z = 391.27 ({[Ni(LCOOH)-H]}$^+$, 100%), 491.27 ({[Ni(LCOOH)]ClO$_4$}$^+$; Anal. Calcd for $C_{18}H_{30}Cl_2N_4NiO_{10}\cdot H_2O$: C 35.44%, H 5.29%, N 9.18%, Ni 9.62%; found: C 35.95%, H 5.56%, N 8.89%, Ni 9.24%.

Synthesis of [Ni(LCONH$_2$)](ClO$_4$)$_2$. To a 30 mL solution of **Lb** (0.20 g, 0.76 mmol) dissolved in MeOH-water (1:1) was added acrylamide (54 mg, 0.76 mmol) in 1 mL of MeOH, and the mixture stirred at 70 °C under N_2 for 24 h. After cooling to RT, the solution was rotavaped to dryness to yield a viscous oil. The oily residue was redissolved in MeOH, treated with Ni(ClO$_4$)$_2\cdot$6H$_2$O (0.28 g, 0.76 mmol) and refluxed for 2 h. After evaporating the solvent, the orange residue was dissolved in MeCN and treated with diethyl ether until the solution turned cloudy. The solution was left undisturbed overnight at RT to yield violet crystals which were filtered and washed with cold EtOH. The product was recrystallized in MeCN-diethyl ether. Yield (0.28 g, 62%); IR (solid): ν (cm^{-1}) = 3439, 3347, 1654, 1601, 1069; ESI-MS(+): m/z = 490.27 ({[Ni(LCONH$_2$)](ClO$_4$)}$^+$, 100%), 390.27 ({[Ni(LCONH$_2$)] − H}$^+$, 15%), 195.73 ({Ni(LCONH$_2$)}$^{2+}$, 60%); Anal. Calcd for $C_{18}H_{31}Cl_2N_5NiO_9\cdot 1.3$MeCN: C 38.39%, H 5.46%, N 13.69%; found: C 38.40%, H 5.48%, N 13.87%.

Synthesis of LCONH$_2$. To a 20 mL aqueous solution of Ni(**LCONH$_2$**)(ClO$_4$)$_2$ (0.35 g, 0.59 mmol) was added NaCN (0.23 g, 4.7 mmol) and stirred at RT for 1 h. The ligand was extracted with $CHCl_3$ (3 × 10 mL). The combined organic layer was washed with brine, dried over Na_2SO_4 then rotavaped to dryness yielding a colorless oil. Yield (0.18 g, 91%); IR (solid): ν (cm^{-1}) = 3233, 1544; ESI-MS(+): m/z = 334.36 ({LCO-NH$_2$+H}$^+$, 100%), 356.36 ({LCONH$_2$+Na}$^+$, 10%); ^{1}H NMR (300 MHz, $CDCl_3$, 300 K): δ=7.56 (t, J=7.8 Hz, 1H), 6.98 (d, J= 7.8 Hz, 2H), 4.94 (br. s, 2H), 3.77 (q, J = 6.9 Hz, 2H), 2.59 (t, J = 6.9 Hz, 2H), 2.51−2.21 (m, 10H), 1.76 (m, 4H), 1.38 (d, J = 6.6 Hz, 6H); ^{13}C NMR (300 MHz, $CDCl_3$, 300 K): δ = 174.61, 163.60, 136.56, 120.70, 59.26, 51.10, 50.04, 45.20, 32.93, 26.98, 23.56.

In several cases, the solvation of the bulk samples (*determined by C,H,N analysis*) *differs from the solvation of additionally recrystallized single-crystalline samples* (*determined by X-ray crystallography*). *The composition of the bulk materials agrees with their IR and NMR spectra.*

Acid−Base Titration of Ni(II)-PyMAC Complexes. The determination of protonation constants was performed by combined spectrophotometric and pH-potentionmetric titration in a modified setup as described by Herrera et al.[17] UV−vis spectra were recorded with a PC2000 CCD array spectrometer equipped with a TP300-UV−vis Transflection Dip Probe (Ocean Optics, Inc.). The pH was measured using an Orion Benchtop Model 420A pH meter equipped with a glass pH/ATC electrode. All measurements were done at 25.0 ± 0.1 °C and ionic strength of 0.10 M KNO_3. In a typical experiment, nickel(II) complexes (0.09 mmol) were dissolved in 15 mL of 0.10 M aqueous KNO_3 solution. Perchloric acid (1.0 M) was added in 1−2 μL portions. UV−vis spectrum and pH of the solution were recorded after each addition. When the UV−vis spectrum no longer changed (usually at pH below 3), the titration was reversed by adding 2−4 μL portions of aqueous KOH solution (2.0 M) until the pH reached 12−12.5. This procedure was tested on [Ni(**LNH$_2$**)](ClO$_4$)$_2$ and gave the value of pK_a = 6.75 ± 0.04, which agrees perfectly with the value obtained by Herrera et al.[17]

Solvent Exchange with [Ni(LCONH$_2$)](ClO$_4$)$_2$. Solid [Ni(**LCONH$_2$**)](ClO$_4$)$_2$ (7.1 mg, 12 μmol) was dissolved in nitromethane (2 mL) and titrated with anhydrous MeCN until the spectrum no longer changes. The final spectrum was compared to the same concentration of [Ni(**LCONH$_2$**)](ClO$_4$)$_2$ prepared in MeCN.

Catalytic Study with ABTS. To an aqueous solution of ABTS (1.8×10^{-4} M) and Ni(II)-PyMAC complex (1.8×10^{-4} M) in 2.0 mL of water was added H_2O_2 (0.072 M). The reaction mixture was stirred, and the absorbance was measured at 414 nm continuously for 20 min at RT.

X-ray Diffraction Studies. The X-ray intensity data for all reported complexes were measured on a Bruker SMART APEX CCD X-ray diffractometer system equipped with a Mo-target X-ray tube (λ = 0.71073 Å). The frames were integrated with the Bruker SAINT software package[25] using a narrow-frame integration

(25) *SAINT*, Version 6.02; Bruker AXS, Inc.: Madison, WI, 2001.

Table 1. Crystallographic Data and Structural Refinement Parameters for [Ni(**LNEt$_2$**)](BH$_3$CN)$_2$, [Ni(**LNEt$_2$**)](ClO$_4$)$_2$, [Ni(**HLNEt$_2$**)](ClO$_4$)$_3$, [Ni(**LCOOH**)](ClO$_4$)$_2$, and [Ni(**LCONH$_2$**)](ClO$_4$)$_2$·CH$_3$CN

	[Ni(**LNEt$_2$**)](BH$_3$CN)$_2$	[Ni(**LNEt$_2$**)](ClO$_4$)$_2$	[Ni(**HLNEt$_2$**)](ClO$_4$)$_3$	[Ni(**LCOOH**)](ClO$_4$)$_2$	[Ni(**LCONH$_2$**)](ClO$_4$)$_2$·CH$_3$CN
formula	$C_{31}H_{55}B_2N_7Ni$	$C_{22}H_{41}Cl_2O_8N_5Ni$	$C_{22}H_{42}Cl_3O_{12}N_5Ni$	$C_{18}H_{32}Cl_2O_{11}N_4Ni$	$C_{22}H_{37}Cl_2O_9N_7Ni$
Fw	606.15	633.21	733.67	610.09	673.20
cryst system	triclinic	triclinic	monoclinic	triclinic	monoclinic
space group	$P\bar{1}$	$P\bar{1}$	$P2_1/c$	$P\bar{1}$	$P2_1/c$
a (Å)	8.6608(7)	8.623(3)	8.6725(13)	9.3224(11)	13.2106(15)
b (Å)	9.3337(8)	9.253(3)	9.3257(14)	11.7217(14)	14.6125(17)
c (Å)	21.7606(18)	18.274(7)	37.872(6)	12.2905(15)	16.2692(19)
α (deg)	79.7840(10)	86.169(6)	90	74.136(2)	90
β (deg)	81.4450(10)	85.052(6)	90.524(2)	81.401(2)	108.913(2)
γ (deg)	83.1300(10)	87.638(6)	90	70.847(2)	90
V (Å^3)	1704.0(2)	1448.4(9)	3062.8(8)	1217.7(3)	2971.0(6)
Z	2	2	4	2	4
T (K)	173(2)	173(2)	173(2)	173(2)	173(2)
λ (Å)	0.71073	0.71073	0.71073	0.71073	0.71073
D_{calc} (g·cm^{-3})	1.181	1.452	1.591	1.664	1.505
μ (mm^{-1})	0.600	0.906	0.963	1.082	0.893
data/restr/par	6290/116/393	6318/10/428	6017/178/484	5478/48/370	6971/0/374
$R1^b$, $wR2^c$	0.0659,	0.0778,	0.0633,	0.0545,	0.0578,
[$I > 2\sigma(I)$]	0.1458	0.1694	0.1664	0.1327	0.1405
$R1^b$, $wR2^c$	0.1205,	0.1220,	0.0795,	0.0754,	0.0745,
(all data)	0.1766	0.1982	0.1759	0.1567	0.1554
quality-of-fit^a	1.022	1.064	1.041	1.027	1.038

^{a} Quality-of-fit $= [\sum[w(F_o^2 - F_c^2)^2]/(N_{obs} - N_{params})]^{1/2}$. ^{b} $R1 = \sum||F_o| - |F_c||/\sum|F_o|$. ^{c} $wR2 = [\sum w(F_o^2 - F_c^2)^2/\sum w(F_o^2)^2]^{1/2}$.

algorithm. The data were corrected for absorption effects using the empirical method (SADABS).[26] The structures were solved by direct methods and refined using the Bruker SHELXTL (Version 6.14) software package.[27] All non-hydrogen atoms in all complexes were refined anisotropically. The oxygen atoms in perchlorate groups in [Ni(**HLNEt$_2$**)](ClO$_4$)$_3$, [Ni(**LNEt$_2$**)](ClO$_4$)$_2$, and [Ni(**LCOOH**)](ClO$_4$)$_2$ were disordered over two rotational orientations, and this disorder was modeled individually in each case. In [Ni(**LNEt$_2$**)](ClO$_4$)$_2$, one of the perchlorate groups showed the whole-body disorder. No disorder of perchlorate anions was observed in [Ni(**LCONH$_2$**)](ClO$_4$)$_2$. Positional disorder of the terminal ethyl groups was modeled over two orientations in [Ni(**LNEt$_2$**)](BH$_3$CN)$_2$ and [Ni(**HLNEt$_2$**)](ClO$_4$)$_3$. Hydrogen atoms were included at idealized positions for structure factor calculations. In [Ni(**LCOOH**)](ClO$_4$)$_2$, water hydrogen atoms were located on a difference Fourier map and refined with restraining equivalent isotropic displacement parameters to be 1.5 times the U_{eq} value of the oxygen atom. Selected crystallographic data for all complexes are summarized in Table 1.

Results and Discussion

Synthesis of Ligands and Nickel(II) Complexes. Our group recently reported modifications to metallomacrocycles bearing an amine pendant arm.[17] The acylation of the amine arm led to dramatic changes in the coordination geometry and spin state of the metal complex. These changes brought about by the transformation of the functional group at the arm inspired us to investigate the effect of other pendant groups to metallomacrocycles. Pendant groups with varying acidity/basicity, or ability to form hydrogen bonds or coordinate to metal ions can also tune catalytic activity of metallomacrocycles and participate in substrate recognition.[5,6,28] Hence, we decided to synthesize three new pyridine-azamacrocycles with pendant arms (**LNEt$_2$**, **LCOOH**, and **LCONH$_2$**) whose properties are compared to previously prepared macrocycles (**LNH$_2$**[17] and **LNHCOMe**[17,24]) (Figure 1). The presence of two alkyl groups at the amine arm of **LNEt$_2$** may affect its ability to coordinate to the metal center compared to **LNH$_2$**. In the case of amide ligands, **LCONH$_2$** and **LNHCOMe**, switching the positions of the C=O and N−H groups relative to the macrocyclic ring may affect not only the coordination of the arm but also its hydrogen bonding property. For **LCOOH**, the pendant arm provides an added feature compared to the amine and amide-containing macrocycles: it is a good proton donor. Carboxylic acid-appended complexes may

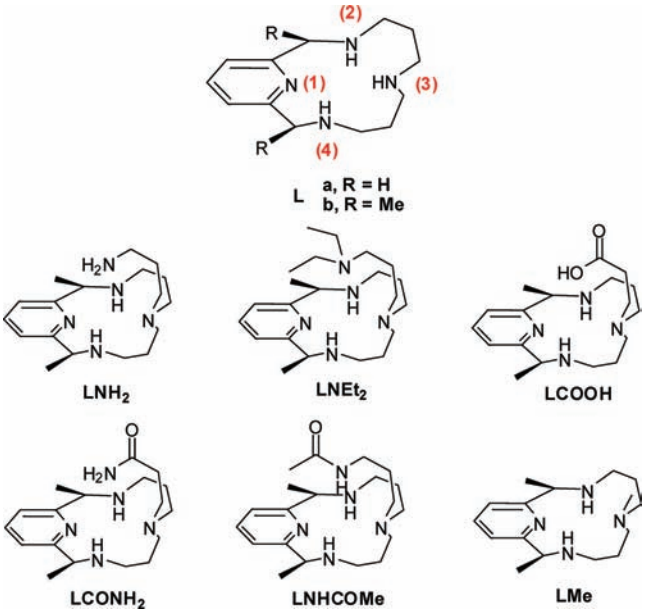

Figure 1. Structures of pyridine-azamacrocycles (PyMACs).

(26) *SADABS*; Bruker AXS, Inc.: Madison, WI, 2001.
(27) Sheldrick, G. M. *SHELXTL*, Version 6.14; University of Göttingen: Göttingen, Germany, 2000.
(28) Costamagna, J.; Ferraudi, G.; Matsuhiro, B.; Campos-Vallette, M.; Canales, J.; Villagrán, M.; Vargas, J.; Aguirre, M. J. *Coord. Chem. Rev.* **2000**, *196*, 125–164.

Scheme 1. Synthesis of New Pyridine-Azamacrocycles $\mathbf{LNEt_2}$, **LCOOH**, and $\mathbf{LCONH_2}$

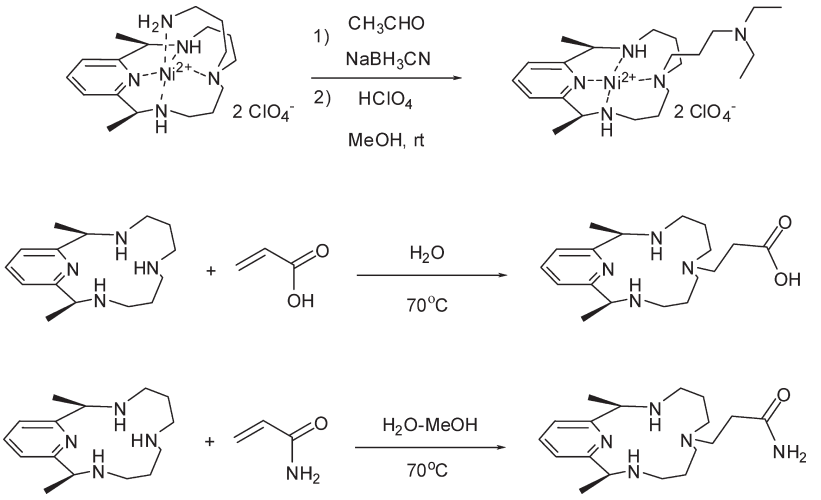

be especially useful in acid-catalyzed or proton-coupled reactions.

Synthesis of pyridine-azamacrocycles with variable pendant arms can be accomplished by selective modification of amino groups either at the macrocyclic ring or at the pendant arm. When the amino groups at the ring are coordinated to the metal ion, they are "protected" from derivatization. This leaves only the amine pendant arm of metallomacrocycles susceptible to reactions such as alkylation or acylation. On the other hand, selective modification of amino groups at the macrocyclic ring can be achieved by free ligands (such as **Lb**[23]) with alkylating reagents (in this case, Michael acceptors) under mild reaction conditions.

Reductive Alkylation of $[Ni(\mathbf{LNH_2})]^{2+}$. Inspired by our recent success in modifying metallomacrocycles through reactions at the pendant amino group to form amide bonds, we decided to apply selective *N*-alkylation to form macrocycles with a tertiary amine arm. Thus, $[Ni(\mathbf{LNH_2})](ClO_4)_2$ was reacted with excess acetaldehyde followed by reduction with $NaBH_3CN$ (Scheme 1). ESI-MS analysis suggested a successful conversion of $[Ni(\mathbf{LNH_2})]^{2+}$ complex into a diethylated product. Both mass and IR spectra also indicated the presence of BH_3CN^- anions and the lack of perchlorate ions in the complex: (a) two intense fragments were found at m/z 514 ($\{[Ni(\mathbf{LNEt_2})](BH_3CN)_2+H\}^+$, 100%) and at m/z 473 ($\{[Ni(\mathbf{LNEt_2})](BH_3CN)\}^+$, 80%), and (b) absorption bands at ν (B−H stretch) = 2371 and 2338 cm^{-1}.[29] Single-crystal X-ray analysis unambiguously showed a nickel(II) complex of $\mathbf{LNEt_2}$ but with BH_3CN^- instead of ClO_4^- as counterions. The two BH_3CN^- anions were found coordinating to the nickel center at the axial positions, while four nitrogen atoms from the macrocycle coordinate at the equatorial positions, forming an octahedral complex. Slowly treating $[Ni(\mathbf{LNEt_2})](BH_3CN)_2$ with $HClO_4$ in MeOH decomposed the cyanoborohydride anions, and produced an orange precipitate. Spectral characterization and X-ray analysis of this compound showed the target complex, $[Ni(\mathbf{LNEt_2})](ClO_4)_2$. The free ligand was obtained by extraction after reacting the $[Ni(\mathbf{LNEt_2})](ClO_4)_2$ complex with NaCN in warm water. ^1H NMR spectrum of the ligand $\mathbf{LNEt_2}$ closely resembled the reported spectrum for $\mathbf{LNH_2}$[17] with additional proton signals at δ = 2.44 ($-CH_2-$) and 0.93 ppm ($-CH_3$) which correspond to the ethyl moiety (see Experimental Section).

These results clearly reveal selective alkylation occurring at the amine pendant arm. No alkylation at other amino groups within the macrocycle was observed. This selective *N*-functionalization of metallomacrocycles can be attributed to the reduced nucleophilicity of amino groups at the macrocycle which are strongly coordinated to the metal ion. The amino group at the pendant arm, on the other hand, is weakly binding and thus susceptible toward alkylation. This synthetic scheme provides a simpler alternative to strategies presented by Kaden[22] and Moore and co-workers[20] in preparing pyridine-azamacrocycles with a tertiary amine arm. This approach may also be useful in bioconjugation of macrocycles with non-hydrolyzable linkers.

Aza-Michael Addition to PyMACs. Unlike azamacrocycles, pyridine-azamacrocycles, **L(a, b)** contain nonequivalent nitrogen atoms which may allow for selective mono-*N*-functionalization. With this ligand, there are two potential sites for *N*-alkylation, namely, the nitrogens close to the pyridine ring (denoted as N2 and N4 in Figure 1) and the middle nitrogen (N3). Alcock, Moore, and co-workers[30] have shown that *N*-alkylation of **La** (R = H) occurs preferentially at N2 and N4. They propose that the lone pairs of these nitrogens are less sterically hindered compared to that of N3. However, there was no report regarding the use of the dialkylated derivative **Lb** (R = Me) for the same reaction. We believe that the presence of two methyl groups close to the pyridine ring can provide the required steric bulk, making the lone pairs of N2 and N4 less available as nucleophiles.

Initially, ethyl bromoacetate was tested as an alkylating agent. However, the reaction with this potent reagent yielded a mixture of products with varying degrees of alkylation. Later, we found that a milder aza-Michael

(29) Berschied, J. R.; Purcell, K. F. *Inorg. Chem.* **1970**, *9*, 624–629.

(30) Alcock, N. W.; Balakrishnan, K. P.; Moore, P.; Pike, G. A. *J. Chem. Soc., Dalton Trans.* **1987**, 889–894.

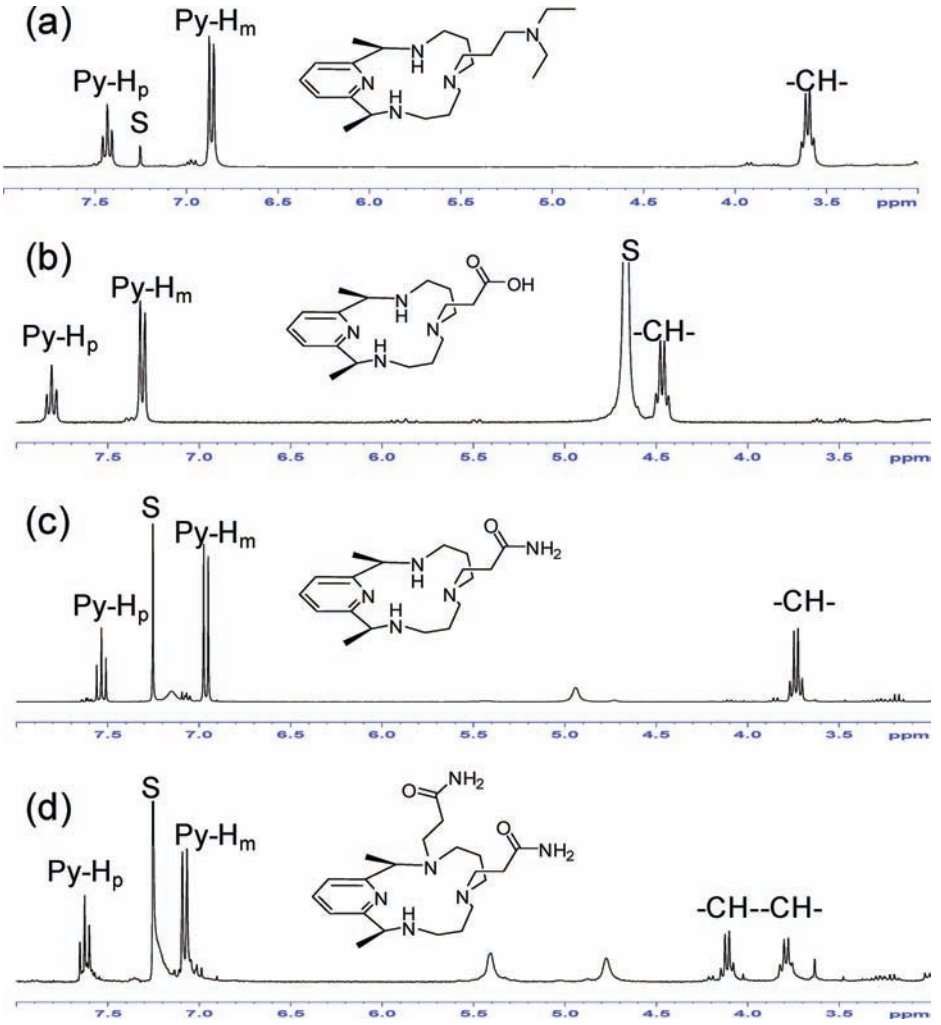

Figure 2. Portion of the ^{1}H NMR spectrum at 300.0 K for (a) **LNEt$_2$** in $CDCl_3$, (b) **LCOOH** in D_2O, (c) **LCONH$_2$** in $CDCl_3$, and (d) **L(CONH$_2$)$_2$** in $CDCl_3$ (S = solvent).

addition of amines to α, β-unsaturated compounds is a simple, convenient, and selective method to prepare monofunctionalized PyMACs. The reaction is run in water, making it an ideal strategy for green chemistry.

When **Lb** was reacted with acrylic acid, only a monoalkylated product was formed, which was isolated after extraction of the unreacted **Lb** from alkaline solution by $CHCl_3$. This simple workup also allows unreacted **Lb** to be recovered and reused.

The simple ^{1}H NMR spectrum of **LCOOH** in D_2O suggests a symmetrical structure, which agrees with the proposed alkylation at the middle nitrogen (N3), as opposed to attack at one of the nitrogens close to the pyridine ring (N2 or N4). The two methylene proton signals, which are sensitive to electronic effects caused by substitution at neighboring nitrogen atoms N2 or N4, are shown as a set of quartets at $\delta = 4.50$ ppm (Figure 2). Similar spectral features were found for **LNEt$_2$**. This result indicates that these protons are equivalent and that the amine nitrogens N2 and N4 were not alkylated. Further structural confirmation of **LCOOH** was provided by crystallographic analysis of its nickel(II) perchlorate complex, which will be discussed later. These results show that aza-Michael addition proceeds preferentially via substitution at the middle secondary amino group. This reaction also represents, to our knowledge, the first example of a regioselective *N*-alkylation of pyridine-azamacrocycles.

Preparation of [Ni(**LCOOH**)]$(ClO_4)_2$ is straightforward. Reacting **LCOOH** with $Ni(ClO_4)_2$ in refluxing methanol yielded an orange product which was recrystallized in acetonitrile-ether mixture. The orange color of the complex is similar to that of four-coordinate [Ni(**LNEt$_2$**)]$(ClO_4)_2$ and the protonated form of [Ni(**LNH$_2$**)]$(ClO_4)_2$, and [Ni(**Lb**)]$(ClO_4)_2$. This suggests that the pendant arm of the **LCOOH** ligand may not be coordinating to the metal ion.

Analogous aza-Michael reaction was performed to synthesize the macrocyclic ligand with an amide pendant arm. Ligand **Lb** was reacted with acrylamide in MeOH-H_2O (1:1) mixture. Electrospray ionization mass spectroscopy (ESI-MS) indicated formation of a monoalkylated adduct as the major product, together with a slight amount of dialkylated product. The monoalkylated ligand **LCONH$_2$** was isolated via fractional crystallization with $Ni(ClO_4)_2$.

^{1}H NMR spectrum of **LCONH$_2$** suggests that alkylation of the macrocycle occurred at the middle amine nitrogen, N3. Similar to **LCOOH**, the methylene proton signals next to the pyridine ring of monoalkylated

Table 2. Selected Bond Lengths (Å) and Angles (deg) for Ni(II)-PyMAC Complexes

atom label	[Ni(**LNEt$_2$**)](BH$_3$CN)$_2$	[Ni(**LNEt$_2$**)](ClO$_4$)$_2$	[Ni(**HLNEt$_2$**)](ClO$_4$)$_3$	[Ni(**LCOOH**)](ClO$_4$)$_2$	[Ni(**LCONH$_2$**)](ClO$_4$)$_2$
Ni(1)−N(1)	1.978(3)	1.876(4)	1.841(4)	1.849(3)	1.988(2)
Ni(1)−N(2)	2.085(4)	1.976(5)	1.947(4)	1.953(4)	2.103(3)
Ni(1)−N(3)	2.106(3)	2.002(4)	1.953(4)	1.971(2)	2.100(2)
Ni(1)−N(4)	2.078(3)	1.972(4)	1.971(4)	1.960(4)	2.099(3)
Ni(1)−N(5)	2.161(4)[a]				2.109(3)[b]
Ni(1)−Other	2.081(4)[a]				2.097(3)[c]
N(1)−Ni(1)−N(2)	81.5(1)	83.6(2)	83.4(2)	84.0(2)	81.2(1)
N(1)−Ni(1)−N(3)	178.8(1)	175.3(2)	176.6(2)	176.5(1)	179.6(1)
N(1)−Ni(1)−N(4)	81.3(1)	83.4(2)	84.0(2)	83.2(1)	80.1(1)
N(1)−Ni(1)−N(5)	84.6(1)				87.7(1)
N(1)−Ni(1)−O(9)					88.3(1)
N(1)−Ni(1)−N(6)	89.6(1)				
N(2)−Ni(1)−N(3)	99.6(1)	96.0(2)	97.0(2)	95.9(1)	98.4(1)
N(2)−Ni(1)−N(4)	161.3(1)	162.9(2)	164.0(2)	163.7(1)	160.4(1)
N(2)−Ni(1)−N(5)	85.4(1)				93.1(1)
N(2)−Ni(1)−N(6)	91.7(1)				
N(2)−Ni(1)−O(9)					91.5(1)
N(3)−Ni(1)−N(4)	97.5(1)	96.1(2)	95.1(1)	96.2(1)	100.3(1)
N(3)−Ni(1)−N(5)	95.3(1)				92.3(1)
N(3)−Ni(1)−N(6)	90.5(1)				
N(3)−Ni(1)−O(9)					91.7(1)
N(4)−Ni(1)−N(5)	85.6(1)				91.8(1)
N(4)−Ni(1)−N(6)	95.6(1)				
N(4)−Ni(1)−O(9)					82.4(1)
N(5)−Ni(1)−N(6)	173.9(1)				
N(5)−Ni(1)−O(9)					173.4(1)

[a] Bonding to N of BH_3CN^- counter ions. [b] Bonding to N of MeCN. [c] Bonding to O of pendant arm.

LCONH$_2$ are equivalent and are shown as a quartet at δ = 3.77 ppm (Figure 2). In the case of dialkylated product, the structure of the macrocycle is no longer symmetrical, hence, the methylene protons are nonequivalent and are split into two sets of quartets at δ = 3.82 and 4.14 ppm.

Crystal Structures of Nickel(II) Complexes. Solid state structures of novel nickel(II) complexes with pendant arms **LNEt$_2$**, **LCOOH**, and **LCONH$_2$** were characterized by X-ray crystallography. Selected bond lengths and angles are listed in Table 2.

The structures of [Ni(**LNEt$_2$**)](BH$_3$CN)$_2$ and [Ni(**LNEt$_2$**)](ClO$_4$)$_2$ are shown in Figure 3. [Ni(**LNEt$_2$**)](BH$_3$CN)$_2$ shows an octahedral geometry about the nickel center with four coordinating nitrogen donors from the ring occupying the equatorial positions while two BH_3CN^- anions occupy the axial positions. The average Ni−N distance of the metal ion to the cyanoborohydride (2.12 Å) is comparable to Ni−N distances from the macrocycle which ranges from 1.98 to 2.11 Å. This shows that the anions bind strongly to the nickel center. In contrast, the same nickel complex of **LNEt$_2$** but with perchlorate counterions exhibits a square planar geometry in which only the four nitrogen atoms from the ring coordinate to the nickel ion. No coordination of either the counterions or the solvent was observed. However, the Ni−O$_{perchlorate}$ distance of ∼2.65 Å suggests a weak electrostatic interaction exists between the metal center and the nearest perchlorate ion (typical Ni−OClO$_3^-$ distances in similar complexes range from 1.95 to 2.15 Å, although very long distances, up to 2.77 Å, were also reported[31]). In both cases, the pendant arm in **LNEt$_2$** does not coordinate to the nickel ion. This is in contrast to structures of [Ni(**LNH$_2$**)](ClO$_4$)$_2$ where the primary amine arm coordinates to the nickel ion at the axial

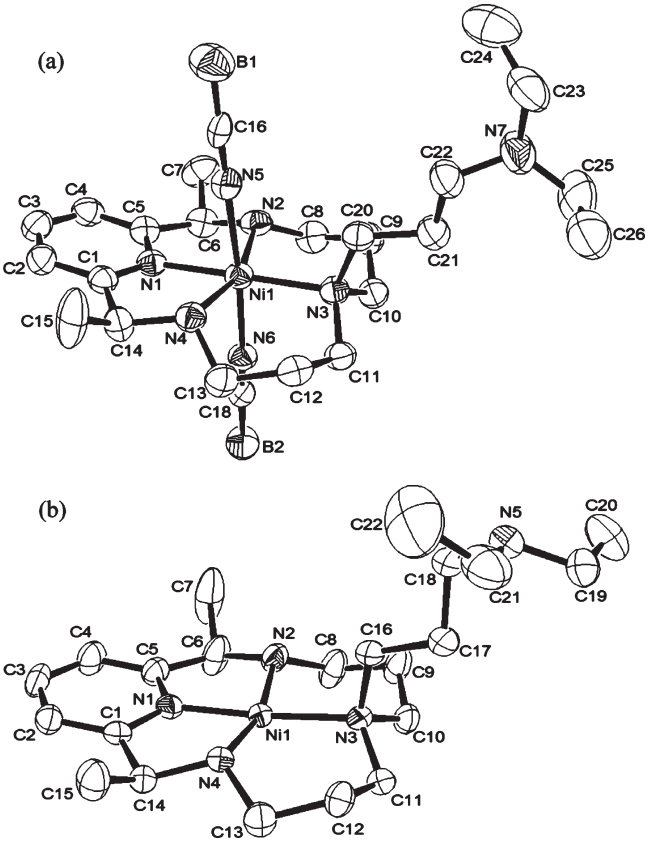

Figure 3. Crystal structures of (a) [Ni(**LNEt$_2$**)](BH$_3$CN)$_2$ and (b) [Ni(**LNEt$_2$**)](ClO$_4$)$_2$ showing 50% probability thermal ellipsoids. Hydrogen atoms and perchlorate ions are omitted for clarity.

(31) Felix, V.; Calhorda, M. J.; Costa, J.; Delgado, R.; Brito, C.; Duarte, M. T.; Arcos, T.; Drew, M. G. B. *J. Chem. Soc., Dalton Trans.* **1996**, 4543–4553.

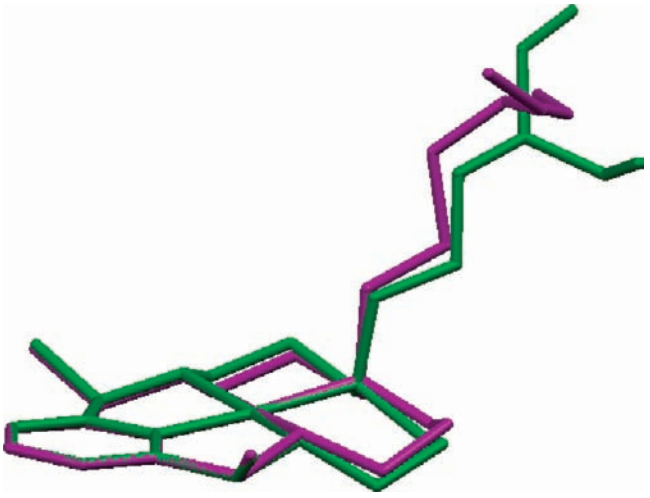

Figure 4. Overlay of X-ray structures of [Ni(**LNEt$_2$**)](ClO$_4$)$_2$ (purple) and its protonated form [Ni(**LHNEt$_2$**)](ClO$_4$)$_3$ (green).

position, resulting in a square pyramidal geometry. Apparently, the two ethyl groups exert steric hindrance toward metal coordination. Examples of nickel(II)macrocycles with *N*-alkylated arms that coordinate to the metal have been previously reported.[19,32] The structure of the complex [Ni(**LNEt$_2$**)](ClO$_4$)$_2$ resembles the protonated form of [Cu(H**LNH$_2$**)](ClO$_4$)$_3$ where the protonated arm is "off" or repelled away from the metal center.[17]

Furthermore, Ni−N distances within the macrocycle are shorter for [Ni(**LNEt$_2$**)](ClO$_4$)$_2$ compared to [Ni(**LNEt$_2$**)](BH$_3$CN)$_2$. A similar behavior has been observed for square planar [Ni(**Lb**)](ClO$_4$)$_2$[33] where ClO_4^- ions do not bind versus octahedral [Ni(**Lb**)](NO$_2$)$_2$[34] where NO_2^- anions bind at the axial positions. This trend is consistent with other reported nickel(II)-azamacrocyclic complexes in which Ni−N bond distances tend to increase when square planar Ni(II) complexes bind axial ligands to form octahedral species.[35] This trend can be attributed to the high spin/low spin electronic configuration of nickel in octahedral or square planar environment, respectively.

Protonation of the pendant arm of [Ni(**LNEt$_2$**)](ClO$_4$)$_2$ led to slight structural changes as shown in Figure 4. Ni−N distances seemed shorter compared to the parent complex. Most noticeable is the bond between Ni and N atom bearing the arm (N3) which is about 0.05 Å shorter in the protonated complex compared to the unprotonated form. Simultaneously, the N−Ni−N bond angles were affected. Again, a noticeable difference can be seen where the Ni−N3−C16 angle of 103.8° in the parent complex is expanded to 105.6° in the protonated form.

The crystal structures of [Ni(**LCOOH**)](ClO$_4$)$_2$ and [Ni(**LCONH$_2$**)](ClO$_4$)$_2$ show that the carboxylic and amide arm was attached to the middle amine nitrogen (N3, Figures 5 and 6). This result suggests that the two methyl groups close to the pyridine ring may be responsible for the preferential attack on this middle nitrogen by providing steric hindrance toward the two nitrogens close to pyridine.

[Ni(**LCOOH**)](ClO$_4$)$_2$ has similar structural features to [Ni(**LNEt$_2$**)](ClO$_4$)$_2$. Both complexes form a four-coordinate square planar structure and have comparable Ni−N distances and N−Ni−N bond angles. The carboxylic acid pendant arm is positioned on the same face of the macrocyclic plane as the methyl groups and both hydrogens at secondary amino groups (N2 and N4). Moreover, the carboxylic acid pendant arm in **LCOOH** does not bind to the nickel ion. This structure is consistent with studies (including structures) of metal complexes with azamacrocycles having an acetic or propionic acid pendant arm which show that the protonated arm does not bind with the metal center whereas the deprotonated form does.[36]

It is also interesting to note that while the carboxylic acid arm does not bind to its metal center, it tends to interact with the nickel ion of a neighboring complex, in the solid state. Crystal packing of [Ni(**LCOOH**)](ClO$_4$)$_2$ shows that a pair of nickel species interact to form a dimeric structure with Ni−O$_{carbonyl}$ distances of about 3.04 Å (Figure 5b). Such complementary formation results from an intermolecular ion-dipole interaction between the nickel ion of one complex and the carbonyl group of the other. A similar "gemini-like" structure was observed in a [Cu(**LNHCOMe**)](ClO$_4$)$_2$[17] complex but with a shorter Ni−O$_{carbonyl}$ distance (2.60 Å) between the pair of copper(II) species.

Unlike [Ni(**LCOOH**)](ClO$_4$)$_2$, the nickel(II) complex of **LCONH$_2$** adopts an octahedral structure, in the presence of CH$_3$CN. Here, the amide pendant arm coordinates via the carbonyl oxygen to the nickel at the axial position. The Ni−O$_{carbonyl}$ distance is about 2.10 Å. An acetonitrile solvent molecule was also found to coordinate at the other axial postion, with the Ni−N (CH$_3$CN) distance of 2.11 Å. The Ni−N distances within the ring are similar to octahedral complexes [Ni(**LNEt$_2$**)](BH$_3$CN)$_2$ and [Ni(**Lb**)](NO$_2$)$_2$.[34] Moreover, **LCONH$_2$** also adopts a conformation similar to **LNEt$_2$** and **LCOOH** where the pendant arm is positioned on the same face of the macrocycle as that of the methyl groups and the secondary amine hydrogens.

"On-Off" Coordination Equilibria of Pendant Arms. The "on" and "off" coordination of pendant arms has been studied by several groups.[17,20,37,38] The different binding modes of the pendant arm toward the metal center is usually driven by changing the pH. For example, we recently found that protonation of [Ni(**LNH$_2$**)]$^{2+}$ results in a structural rearrangement from a five-coordinate square pyramidal to a four-coordinate square planar geometry.[17] The dissociation of the coordinated amine arm occurs in slightly acidic media (pK_a = 6.75). The arm "on" and "off" reversible process also results in a dramatic color change from blue to orange, respectively. UV−vis titration of the complex shows the disappearance of absorption bands at 368 and 571 nm and the appearance

(32) Fabbrizzi, L.; Licchelli, M.; Pallavicini, P.; Parodi, L. *Angew. Chem., Int. Ed.* **1998**, *37*, 800–802.
(33) Dewar, R.; Fleischer, E. *Nature* **1969**, *222*, 372–373.
(34) Drew, M. G. B.; Hollis, S. *Acta Crystallogr., Sect. B* **1980**, *36*, 1944–1947.
(35) Meyer, F.; Kozlowski, H. In *Comprehensive Coordination Chemistry II*; McCleverty, J. A., Meyer, T. J., Eds.; Elsevier Inc.: San Diego, CA, 2004; Vol. *6*, pp 386−390.
(36) Kaden, T. A. *Pure Appl. Chem.* **1993**, *65*, 1477–1483.
(37) Lotz, T. J.; Kaden, T. A. *J. Chem. Soc., Chem. Commun.* **1977**, 15–16.
(38) Schiegg, A.; Kaden, T. A. *Helv. Chim. Acta* **1990**, *73*, 716–722.

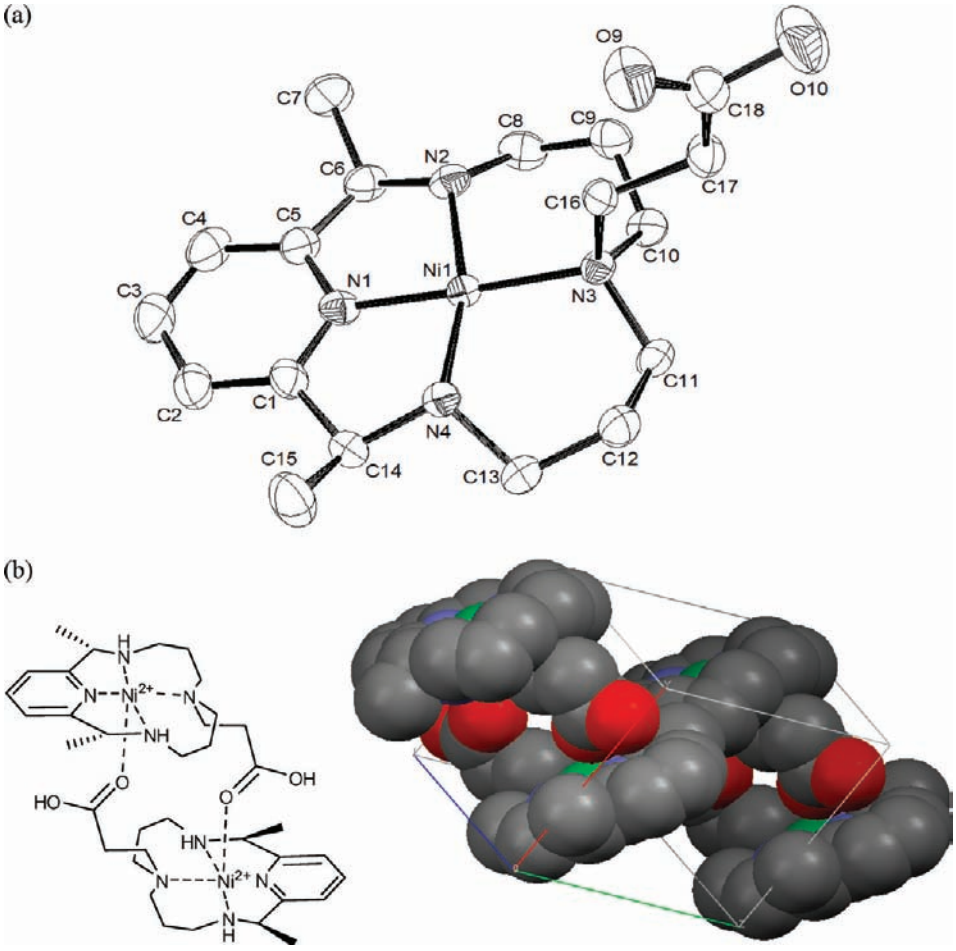

Figure 5. (a) Crystal structure of [Ni(**LCOOH**)]$(ClO_4)_2$ showing 50% probability thermal ellipsoids. Hydrogen atoms and perchlorate ions are omitted for clarity. (b) Ion-dipole interaction between two nickel complexes.

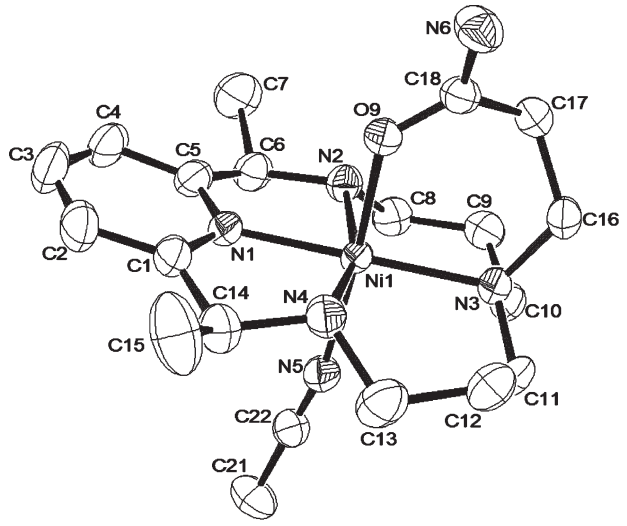

Figure 6. Crystal structure of [Ni(**LCONH$_2$**)]$(ClO_4)_2$ showing 50% probability thermal ellipsoids. Hydrogen atoms and perchlorate ions are omitted for clarity.

of a band at 472 nm, upon protonation. These results indicate that the complex is high-spin when the arm is "on" and low spin when the arm is "off."[17,18]

Spectral changes were also observed during the acid−base titration of aqueous solutions of nickel(II) complexes with ligands **LNEt$_2$**, **LCOOH**, **LCONH$_2$**, and **LNHCOMe** (Figure 7). Results indicate the presence of one ionizable proton in the protonated form of each compound. Acid dissociation constants (pK_a) of the pendant arm in all Ni(II)-PyMAC complexes are lower compared to analogous organic compounds (Table 3). This increased acidity of pendant arms can be attributed to (a) stability of the conjugate base form of the arm because of coordination to the nickel center, and (b) relative destabilization of the acid form because of electrostatic repulsion between the nickel ion and the positively charged arm, as in the case of protonated amine arms. For [Ni(**LNH$_2$**)]$^{2+}$, both the electrostatic repulsion between Ni^{2+} and $-NH_3^+$ arm and the favorable coordination of the $-NH_2$ arm (as mentioned previously) may be responsible for its enhanced acidity versus propylamine by 4 orders of magnitude.[15,17,20,37,38]

In the case of [Ni(**LNEt$_2$**)]$^{2+}$, the *N*-dialkylated arm inhibits potential coordination to the nickel ion. Reversible protonation of the arm still occurs but without structural rearrangement. UV−vis spectra of the acid−base titration of [Ni(**LNEt$_2$**)]$^{2+}$, together with crystal structures, reveal minimal effect on the structure of the complex. Small variation in Ni−N bond distances in the macrocycle upon protonation may account for the observed spectral changes. In the absence of the arm coordination to the metal center, the 10-fold increase in

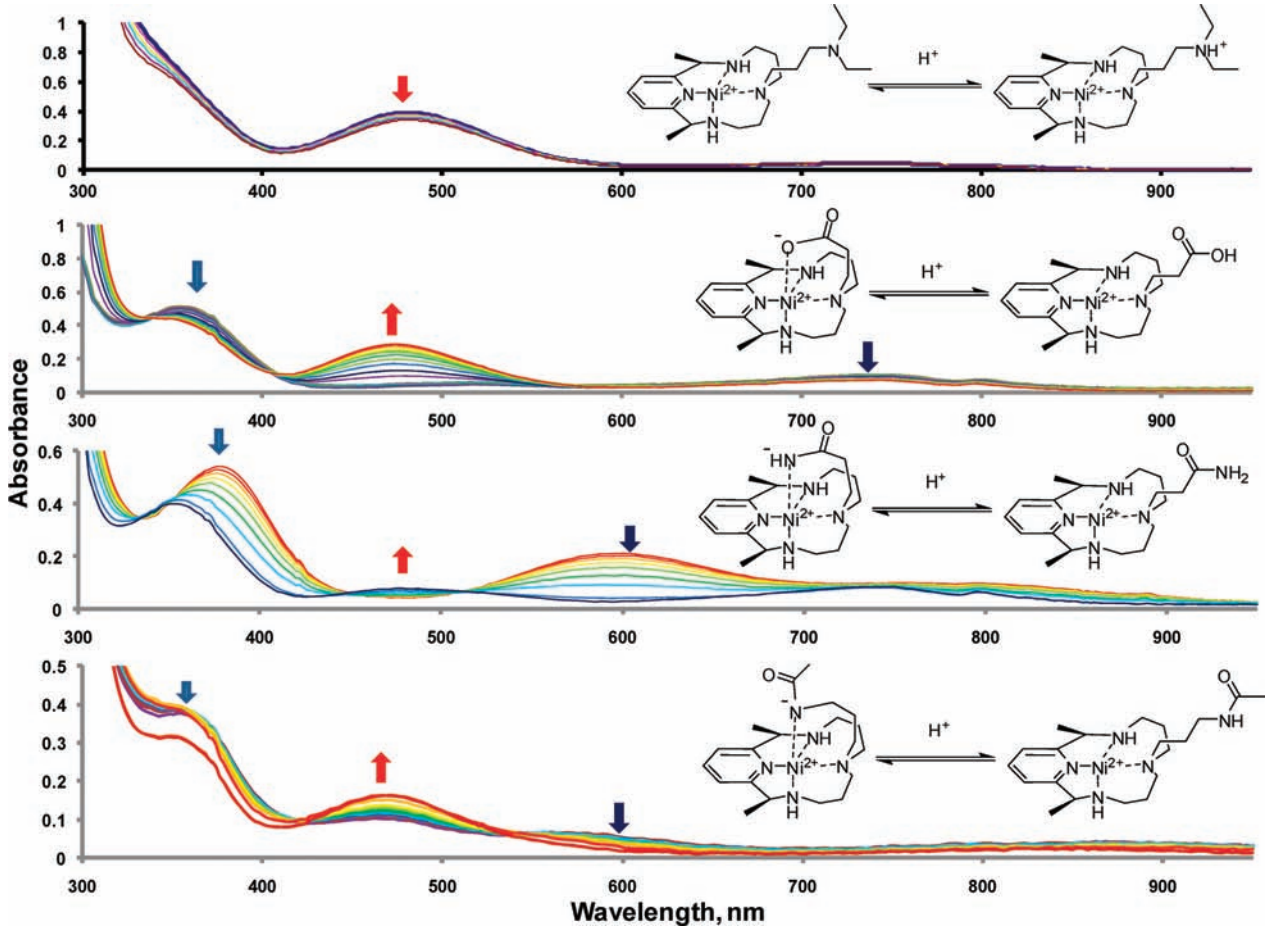

Figure 7. UV−vis spectral changes upon protonation of nickel(II) complexes. Conditions: 1−2 μL portions of $HClO_4$ (1.0 M) were added to Ni(II)-PyMAC (6.0 mM) at 25.0 ± 0.1 °C and I = 0.10 M KNO_3.

Table 3. Acid Dissociation Constants of Ni(II)-PyMAC Complexes and Organic Compounds with Analogous Functional Groups in Aqueous Solution

$[Ni(PyMAC)]^{2+}$ complex	equilibrium constant (pK_a)		compound
$[Ni(\mathbf{LNH_2})](ClO_4)_2$[17]	6.75 ± 0.04	10.71[39]	$PrNH_2$
$[Ni(\mathbf{LNEt_2})](ClO_4)_2$	9.36 ± 0.04	10.78[39]	Et_3N
$[Ni(\mathbf{LCOOH})](ClO_4)_2$	3.03 ± 0.04	4.88[39]	CH_3CH_2COOH
$[Ni(\mathbf{LCONH_2})](ClO_4)_2$	11.36 ± 0.02	15.1 (25.5, DMSO)[40]	CH_3CONH_2
$[Ni(\mathbf{LNHCOMe})](ClO_4)_2$[24]	11.30 ± 0.04	(25.9, DMSO)[40]	$CH_3CONHCH_3$

Table 4. UV-vis Spectra of Ni(II) Macrocyclic Complexes

	absorption bands, λ_{max} nm (ε/M^{-1} cm^{-1})		
complex	MeCN	pH 3.0	pH 10.0
$[Ni(\mathbf{LNH_2})](ClO_4)_2$[17]	364 (150), 568 (51), 810 (16), 884 (12)	472 (85)	368 (143), 571 (53), 812 (20), 885 (13)
$[Ni(\mathbf{LNEt_2})](ClO_4)_2$	478 (73), 738 (11), 802 (9)	350 (37), 470 (22), 748 (3), 794 (3)	350 (55), 470 (32), 742 (11), 794 (11)
$[Ni(\mathbf{LCOOH})](ClO_4)_2$	342 (111), 490 (29), 730 (24), 800 (17)	348 (73), 476 (48), 738 (12), 794 (8)	354 (85), 520 (9), 742 (16), 800 (12)
$[Ni(\mathbf{LCONH_2})](ClO_4)_2$	355 (79), 505 (8), 737 (18), 799 (12)	354 (66), 476 (13), 746 (14), 796 (11)	378 (90), 602 (35), 744 (16), 798 (16)
$[Ni(\mathbf{LNHCOMe})](ClO_4)_2$[24]	360 (462), 464 (122), 744 (12)	348 (52), 470 (27), 854 (4)	354 (63), 558 (10), 856 (6), 884 (6)

acidity over metal-free triethylamine (Table 3) is entirely due to electrostatic destabilization of the protonated arm by the positively charged nickel(II) center located nearby. The protonation constant for $[Ni(\mathbf{LNEt_2})]^{2+}$ is higher (pK_a = 9.36) compared to that of a similar nickel(II) aminopyridine macrocycle with an *N*,*N*-dimethylethylamino arm (pK_a = 6.29).[37] The latter ligand has a shorter pendant arm and is able to coordinate to the metal ion, whereas $\mathbf{LNEt_2}$ has a longer arm and is non-coordinating. Thus, the difference in basicity can also be attributed to favorable arm coordination of the ligand with a shorter arm versus the ligand with a longer arm.[38] This trend was also observed by Alcock, Moore, and co-workers[19] with macrocycles containing pyrrolidinyl groups with varying arm length.

Changing the pH of an aqueous solution of $[Ni(\mathbf{LCOOH})]^{2+}$ from pH 2 to 12 resulted in a decrease in absorbance around 450−520 nm and an increase in

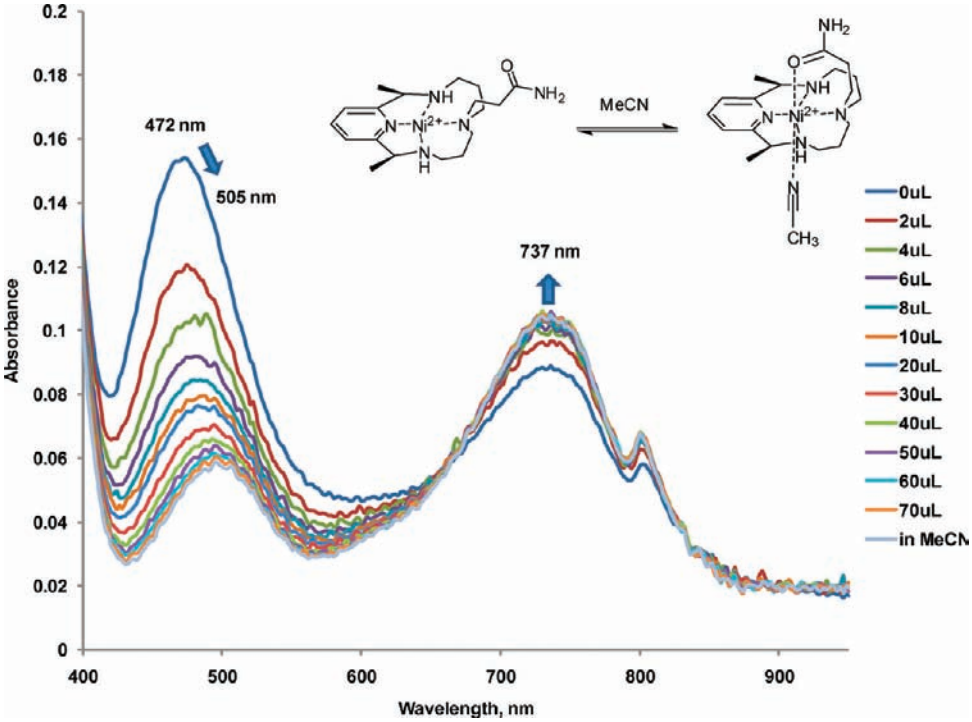

Figure 8. UV−vis titration of [Ni(**LCONH$_2$**)](ClO$_4$)$_2$ in nitromethane with acetonitrile.

absorbance close to 350 nm. The shift in λ_{max} from 420 nm in acidic solution to 520 nm in alkaline solution may indicate coordination of the carboxylate group to the nickel center after deprotonation of the arm. Moreover, it appears that the band at 476 nm belongs to a low-spin form of the complex, while the bands at ~350 and 520 nm originate from the high-spin form. Similar spectral features have been observed in low spin to high spin conversion for metal complexes of azamacrocycles with pendant arms.[15,16,22,37,38] The calculated protonation constant of [Ni(**LCOOH**)]$^{2+}$ (pK_a = 3.03) is within range for reported carboxylic acid-bearing azamacrocycles[16] and is lower than the pK_a's of aliphatic carboxylic acids.

For [Ni(**LCONH$_2$**)]$^{2+}$, a dramatic color change from light orange in slightly acidic or neutral solution to blue-green in alkaline solution is observed. Upon addition of base to the aqueous solution of [Ni(**LCONH$_2$**)]$^{2+}$, the UV−vis spectrum changed: the absorption band at 476 nm disappeared, and the band at 602 nm grew in. Similar spectral changes were observed for [Ni(**LNHCOMe**)]$^{2+}$, in which the pendant arm also bears an amide functionality but with the amide nitrogen atom placed between the carbonyl carbon and the alkyl linker. Adding a base to this complex resulted in a decrease in absorbance at 470 nm and an increase in absorbance at 558 nm. In both complexes, the band at 354 and 348 nm, respectively, also increased and shifted to longer wavelengths. These results indicate deprotonation of the amide arm accompanied by coordination of the arm to nickel. The λ_{max} shift to longer wavelengths (550−600 nm) also suggests that "on" coordination of the arm leads to structural and electronic changes from a low-spin, square planar complex to a high-spin, octahedral complex.[12] In this case, the deprotonated amide N, rather than the carbonyl O, coordinates to the nickel ion.[41,42] Calculated pK_a for both complexes was found to be 11.3. This value is close to the reported protonation constant for Cu(II)-azamacrocyclic complex with an amide pendant arm (pK_a = 10.98).[42]

We also observe that the color and the visible spectrum of [Ni(**LCONH$_2$**)](ClO$_4$)$_2$ depends on the solvent used. In MeCN, the complex is blue-violet while in other solvents such as water, methanol, or nitromethane, it is orange. Other carbonyl-containing ligands such as **LCOOH** and **LNHCOMe** do not exhibit this behavior. The color change can be followed by UV−vis titration (Figure 8). Slow addition of anhydrous MeCN to [Ni(**LCONH$_2$**)](ClO$_4$)$_2$ in MeNO$_2$ resulted in a decrease in absorbance at 472 nm with a shift to 505 nm. This spectral shift is accompanied by an increase in absorbance at 737 nm with an isosbestic point at 670 nm. This observation indicates that MeCN can also induce structural rearrangement of the complex. Thus, in nitromethane, the complex exists mostly in the square planar form with the arm "off" as indicated by its color and spectral features, while coordination of MeCN causes the arm to also coordinate to the metal and form an octahedral complex as shown by crystal structures. This result implies that MeCN coordinates to the nickel center in [Ni(**LCONH$_2$**)](ClO$_4$)$_2$ better than water, methanol, or nitromethane. Mixing acetamide with a nickel complex lacking a −CONH$_2$ arm such as [Ni(**LMe**)](ClO$_4$)$_2$ in MeCN did not show spectral features analogous to [Ni(**LCONH$_2$**)](ClO$_4$)$_2$. This suggests that acetamide and MeCN did not coordinate to the [Ni(LMe)]$^{2+}$ at the axial positions to form an octahedral

(39) *Handbook of Physical Properties of Organic Chemicals*; Howard, P. H., Meylan, W. M., Eds.; CRC Press: Boca Raton, FL, 1997.
(40) Bordwell, F. G. *Acc. Chem. Res.* **1988**, *21*, 456–463.
(41) Schibler, W.; Kaden, T. A. *J. Chem. Soc., Chem. Commun.* **1981**, 603–604. Zuberbühler, A.; Kaden, T. *Helv. Chim. Acta* **1972**, *55*, 623–629.
(42) Siegfried, L.; Comparone, A.; Neuburger, M.; Kaden, T. A. *Dalton Trans.* **2005**, 30–36.

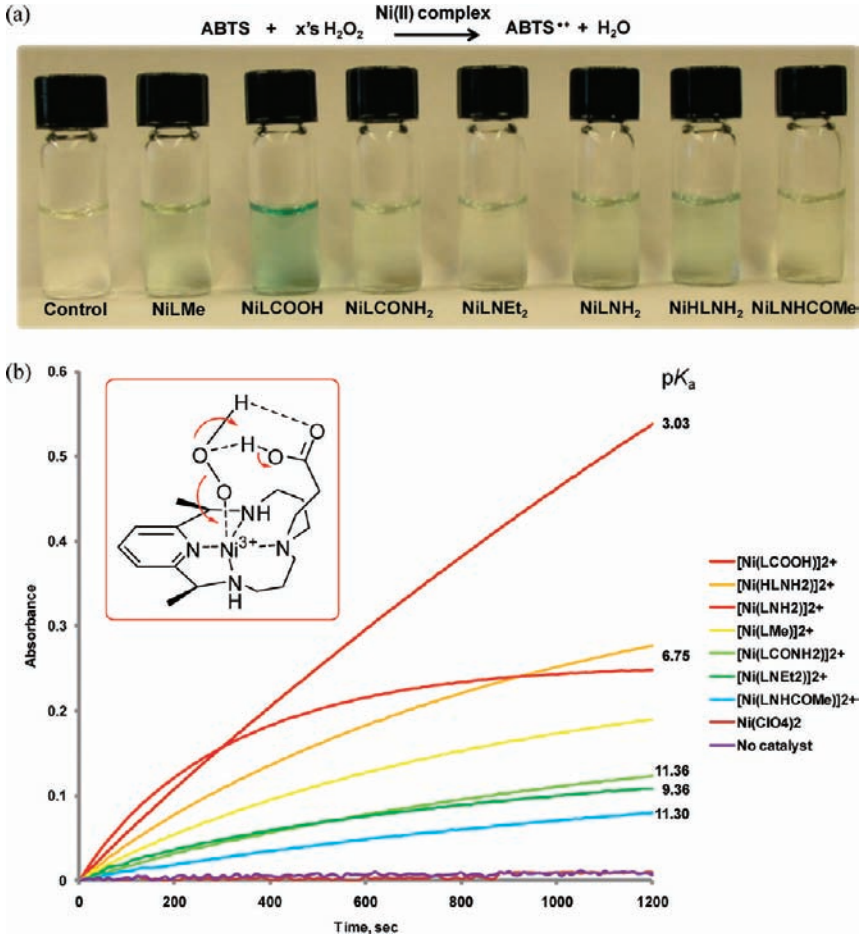

Figure 9. Catalytic oxidation of ABTS with H_2O_2. Reaction mixture: ABTS (1.8×10^{-4} M), H_2O_2 (0.072 M), Ni(II) complex (1.8×10^{-4} M) in H_2O (2 mL). (a) Photo of reaction mixtures taken after 30 min reaction. (b) Absorbance versus time plot of catalytic oxidation of ABTS with H_2O_2. Absorbance was measured at 414 nm continuously for 20 min at RT. Inset: Proposed activation of H_2O_2 with $[Ni(\mathbf{LCOOH})]^{2+}$ complex.

complex similar to $[Ni(\mathbf{LCONH_2})](ClO_4)_2$. Hence, binding of the $-CONH_2$ group and MeCN occurs when the amide group is attached to metallomacrocycles. The synergistic binding of a pendant arm with coordinating solvents has also been thought to occur in azamacrocycles bearing $-CH_2CH_2OH$ and $-CH_2OCH_3$ arms in MeCN.[43,44] It has been suggested that weak interactions between the pendant arm and MeCN led to the solvent's strong coordinating ability compared to water.[45] Moreover, a chelate effect brought about by the favorable coordination of the arm made it easier for MeCN molecules to coordinate as well.[44,46] This interesting behavior of $[Ni(\mathbf{LCONH_2})](ClO_4)_2$ might be useful in modulating properties of the complex as the arm "on-off" coordination can be accomplished by changing solvents or by providing other electronically complementary monodentate axial ligands.

Peroxidase-Like Catalytic Study. Nickel(II) complexes are known to catalyze the oxidation of various substrates such as DNA, alkenes, organic and inorganic anions in aqueous solutions or phase-transfer conditions.[47] Thus, we decided to screen our nickel complexes to act as oxidation catalysts to show preliminary evidence for the effect of varying pendant groups on its catalytic property. Unexpectedly, we found the compound 2,2′-azino-bis(3-ethylbenzthiazoline-6-sulfonic acid) (ABTS) to be a good substrate for this purpose (Figure 9a). ABTS, which undergoes a one-electron oxidation to form a green-colored cation radical (λ_{max} = 414 nm, $\varepsilon = 3.6 \times 10^4$ M^{-1} cm^{-1}),[48] is commonly used as a substrate to study peroxidase-like activity of synthetic enzymes (usually iron-containing complexes).[49]

Nickel(II) complexes of pyridine-azamacrocycles with pendant arms were shown to catalyze the oxidation of ABTS using H_2O_2 as oxidant, with varying rates of reaction (Figure 9b). Neither $Ni(ClO_4)_2$ alone nor pure ligands showed any catalysis. Thus, it is necessary to have a bound Ni^{2+} ion in the macrocyclic ligand to exhibit

(43) Kang, S.-G.; Kweon, J. K.; Jeong, G. R.; Lee, U. *Bull. Korean Chem. Soc.* **2008**, *29*, 1905–1910.
(44) Kang, S.-G.; Ryu, K.; Song, J. *Polyhedron* **1999**, *18*, 2193–2199.
(45) Iwamoto, E.; Yokoyama, T.; Yamasaki, S.; Yabe, T.; Kumamaru, T.; Yamamoto, Y. *J. Chem. Soc., Dalton Trans.* **1988**, 1935–1941. Okano, K.; Tsukube, H.; Hori, K. *Tetrahedron* **2005**, *61*, 12006–12011.
(46) Kang, S.-G.; Choi, J.-S.; Kim, S.-J. *Bull. Korean Chem. Soc.* **1995**, *16*, 518–523.
(47) Bhattacharya, S.; Saha, B.; Dutta, A.; Banerjee, P. *Coord. Chem. Rev.* **1998**, *170*, 47–74. Zilbermann, I.; Maimon, E.; Cohen, H.; Meyerstein, D. *Chem. Rev.* **2005**, *105*, 2609–2626.
(48) Childs, R. E.; Bardsley, W. G. *Biochem. J.* **1975**, *145*, 93–103.
(49) Choma, C. T.; Schudde, E. P.; Kellogg, R. M.; Robillard, G. T.; Feringa, B. L. *J. Chem. Soc., Perkin Trans. 1* **1998**, 769–773. Organo, V. G.; Ye, W.; Agarwal, P. K.; Rybak-Akimova, E. V. *J. Incl. Phenom. Macrocycl. Chem.* **2009**, *64*, 15–21. Yamaguchi, H.; Tsubouchi, K.; Kawaguchi, K.; Horita, E.; Harada, A. *Chem.—Eur. J.* **2004**, *10*, 6179–6186. Zhang, X.; Zhang, D.; Busch, D. H.; Eldik, R. v. *J. Chem. Soc., Dalton Trans.* **1999**, 2751–2758.

catalytic activity. Among the complexes with carbonyl pendant arms, [Ni(**LCOOH**)]$(ClO_4)_2$ showed the highest catalytic activity, while those with amide functional groups were less active. Nickel complex of amine-bearing ligand **LNH$_2$** also fared better than the dialkylated amine **LNEt$_2$**. Moreover, protonation of [Ni(**LNH$_2$**)]$^{2+}$ enhanced its catalytic activity and extended its lifetime. These results clearly show differences in catalytic activity which can be attributed to functional groups with varying hydrogen bonding and proton-donating abilities at the pendant arm of the ligand. One possible scenario is that the pendant arm interacts with the peroxide via hydrogen bonding. Thus, [Ni(**LNH$_2$**)]$^{2+}$, which can form more hydrogen bonds with the peroxide, performs better than [Ni(**LNEt$_2$**)]$^{2+}$. This scenario, however, does not fully account for the differences in catalytic activity between carbonyl-containing pendant arms ([Ni(**LCOOH**)]$^{2+}$, [Ni(**LCONH$_2$**)]$^{2+}$, and [Ni(**LNHCOMe**)]$^{2+}$) which all possess relatively similar hydrogen bonding properties. Therefore, other factors should be considered. The activation of H_2O_2 may also involve an intramolecular proton transfer between the pendant arm and the coordinated peroxide, which facilitates peroxide O−O bond cleavage (Figure 9b inset). This "pull effect" is similar to a proton-coupled electron transfer reaction observed for H_2O_2 activation by "hangman" metalloporphyrins bearing an appended carboxylate group.[6,8] Results of the catalytic study seem to correlate with the protonation constant of the nickel complex. Thus, complexes with acidic or slightly acidic ($pK_a < 7$) pendant arms such as [Ni(**LCOOH**)]$^{2+}$ and [Ni(**LNH$_2$**)]$^{2+}$ showed high reactivity. In contrast, complexes with basic ($pK_a > 7$) pendant arms like [Ni(**LNEt$_2$**)]$^{2+}$, [Ni(**LCONH$_2$**)]$^{2+}$, and [Ni(**LNHCOMe**)]$^{2+}$ showed low reactivity and were comparable with each other (Figure 9b).

We also found that [Ni(**LNH$_2$**)]$(ClO_4)_2$ reacted slightly faster than [Ni(**LCOOH**)]$(ClO_4)_2$ at the beginning but tended to slow down after 1000 s. Perhaps the amine arm of [Ni(**LNH$_2$**)]$^{2+}$ may have acted as a Lewis base in activating H_2O_2 by promoting peroxide coordination to the nickel(II) center. Base-driven activation of hydrogen peroxide has been implicated in epoxidation of olefins by hydrogen peroxide with Mn(II)-porphyrin systems and nitrogeneous bases as cocatalyst.[50] However, the catalytic activity of [Ni(**LNH$_2$**)]$^{2+}$ is short-lived, which may be due to the relative ease in oxidizing the $-NH_2$ moiety compared to −COOH group at the arm. Other factors, including (but not limited to) stability of Ni(II)-PyMAC complexes during oxidation and/or formation of free radical species[51] may have also played a role in the oxidation of ABTS. Nonetheless, the catalytic activity of nickel PyMACs seem to be modulated by functional groups of the pendant arm. Thus, detailed studies on the mechanism of peroxide activation of these metallomacrocycles with pendant arms are warranted and are being conducted in our laboratory.

Conclusions

Novel nickel(II) complexes of pyridine-azamacrocycles (PyMACs) with pendant arms have been prepared and characterized. Simple, direct, and selective mono-functionalization of PyMACs can be accomplished either by derivatization at the pendant arm of metal complexes or by utilizing Michael addition reaction on free ligands. Nickel(II)-PyMAC complexes with a flexible pendant arm exhibit structural and color changes due to "on-off" arm coordination to the metal center. These changes can be induced by varying the pH of the solution or changing the solvent. Pendant arms with varying hydrogen bonding and proton-donor properties have shown to affect the peroxidase-like activity of Ni(II)-PyMAC complexes in the oxidation of ABTS with hydrogen peroxide. Further investigation on the effect of pendant arms on properties of other redox-active metal complexes are being undertaken in our laboratory. Moreover, new synthetic methodologies presented here can be used to prepare a wide range of macrocyclic ligands with mono-functionalized pendant arms, and potentially macrocyclic ligands with multifunctional groups.

Acknowledgment. This work was supported by the U.S. Department of Energy (Grant DE-FG02-06ER15799 to E.R.A.). The NMR facility, the kinetic instrumentation, and the ESI-MS spectrometer at Tufts were supported by the NSF Grants CHE-MRI 0821508, CHE-CRIF 0639138, and CHEM-MRI 0320783. A.F. is very grateful to the University at Albany for supporting the X-ray center at the Department of Chemistry. The authors thank Wanhua Ye for helpful discussions.

Supporting Information Available: X-ray crystallographic data in CIF format for all the structures reported in this paper. This material is available free of charge via the Internet at http://pubs.acs.org.

(50) Battioni, P.; Renaud, J. P.; Bartoli, J. F.; Reina-Artiles, M.; Fort, M.; Mansuy, D. *J. Am. Chem. Soc.* **1988**, *110*, 8462–8470. Jones, C. W. *Applications of Hydrogen Peroxide and Derivatives*; The Royal Society of Chemistry: Cambridge, U.K., 1999.

(51) Brodovitch, J. C.; McAuley, A.; Oswald, T. *Inorg. Chem.* **1982**, *21*, 3442–3447. Ueda, J.-i.; Ozawa, T.; Miyazaki, M.; Fujiwara, Y. *Inorg. Chim. Acta* **1993**, *214*, 29–32.